



This is the peer reviewed version of the following article: Gaiani, Greta, María Rey, Àngels Tudó, Maria Rambla, Jorge Diogène, Mònica Campàs, and Carles Alcaraz. 2022. "New Information About The Toxicological Profile Of Prorocentrum Panamense (Prorocentrales , Dinophyceae) And Its Global Distribution". *Phycological Research*. doi:10.1111/pre.12479., which has been published in final form at <https://doi.org/10.1111/pre.12479>. This article may be used for non-commercial purposes in accordance with Wiley Terms and Conditions for Use of Self-Archived Versions <http://www.wileyauthors.com/self-archiving>.

Document downloaded from:



1 **New information about the toxicological profile of**
2 ***Prorocentrum panamense* (Prorocentrales, Dinophyceae) and its**
3 **global distribution**

4 Greta Gaiani^{*}, María Rey, Àngels Tudó, Maria Rambla, Jorge Diogène, Mònica
5 Campàs, Carles Alcaraz^{*}

6

7 IRTA, Marine and Continental Waters, Ctra. Poble Nou km 5.5, 43540 Sant Carles de la
8 Ràpita, Spain

9

10 ^{*}To whom correspondence should be addressed.

11 Email: greta.gaiani@irta.cat; carles.alcaraz@irta.cat

12

13 **SUMMARY**

14 Dinoflagellates of the genera *Prorocentrum* and *Dinophysis* are known producers of toxic
15 compounds belonging to the okadaic acid (OA) group. The ingestion of shellfish
16 contaminated with these toxins cause a human disease named diarrhetic shellfish
17 poisoning (DSP). In this study, the first record of *Prorocentrum panamense*, a potential
18 toxin-producer species, was reported in the Canary Islands together with its toxicological
19 characterization. *Prorocentrum panamense* cells were collected during April 2017 from
20 natural pools located in the Northeastern part of Gran Canaria. This new record represents
21 an expansion of *P. panamense* distribution area, previously restricted to the Pacific
22 Ocean, Indian Ocean, Arabian Gulf and the Caribbean, and its introduction mechanisms
23 is discussed. Laboratory cultures of *P. panamense* were settled and toxin production was
24 assessed in both cell pellets and culture media at four different growth phases (latency,
25 exponential, early stationary and late stationary) implementing LC-MS/MS and neuro-2a
26 cell-based assay (CBA). LC-MS/MS allowed the identification of OA in the fraction
27 corresponding to the late stationary phase, and tests performed on neuro-2a cells showed,
28 for most of the fractions, OA-like activity observable by both cell morphology changes
29 and cell mortality. This information is fundamental for a better understanding of the genus
30 *Prorocentrum* global distribution, its ecology and risks associated to toxic producing
31 species.

32 **Keywords:**

33 Cell-based assay (CBA), central eastern Atlantic Ocean, diarrhetic shellfish poisoning
34 (DSP), okadaic acid (OA), *Prorocentrum panamense*, toxin production.

35 INTRODUCTION

36 Diarrheic shellfish poisoning (DSP) is a foodborne disease reported in several areas
37 worldwide (Gestal *et al.* 2008). It is associated with the consumption of bivalves
38 contaminated with toxins of the okadaic acid (OA) group, mainly produced by
39 dinoflagellates of the genera *Prorocentrum* and *Dinophysis* (Yasumoto *et al.* 1985).
40 Before implementing efficient monitoring programs, DSP outbreaks affected a large
41 number of people, causing the closing of shellfish harvesting areas even for several
42 months (Economou *et al.* 2007), resulting in dramatic losses in both the aquaculture and
43 fisheries sectors. The toxins responsible for DSP include OA, dinophysistoxin-1 (DTX-
44 1) and dinophysistoxin-2 (DTX-2). Their mechanism of action is based on phosphatase
45 inhibition, which can interfere with several mammalian physiological processes, such as
46 the cell cycle regulation and the metabolism of intracellular protein, potentially causing
47 the inflammation of the intestinal tract (i.e., abdominal pain, vomiting) and diarrhea
48 (Yasumoto *et al.* 1985). Furthermore, OA and DTX-1 have tumor promoting activity
49 (Fujiki *et al.* 1991). Currently, the genus *Prorocentrum* is composed of 80 species,
50 divided among planktonic and epibenthic species (Hoppenrath *et al.* 2013). Furthermore,
51 the taxonomic status of some species is in flux, because the *Prorocentrum* genus presents
52 a large variety in terms of cell shape, length and width, number and shape of lateral plates
53 and marginal pores, thus making difficult species identification with microscope
54 techniques (Aligizaki *et al.* 2009). Recent progress in molecular techniques has improved
55 species identification and has contributed to the clarification of taxonomy of this genus.
56 Currently, within the genus, six planktonic and nine epibenthic species form high-
57 biomass blooms and are considered potentially harmful (Glibert *et al.* 2012). Among the
58 six planktonic species, only *Prorocentrum minimum* (Pavillard) Schiller has been
59 described as potentially toxic (Grzebyk *et al.* 1998; Glibert *et al.* 2012). Instead, all the

60 benthic species have been described as toxic, with *Prorocentrum lima* (Ehrenberg)
61 F.Stein being the most toxic (Moreira-González *et al.* 2018). However, since the genus
62 *Prorocentrum* counts a huge number of species, it is probable that there may be more
63 unidentified harmful species in addition to the currently described (Glibert *et al.* 2012).
64 Some species of the genus *Prorocentrum* have a global distribution, such as
65 *Prorocentrum emarginatum* Y. Fukuyo, *Prorocentrum mexicanum* Osorio-Tafall,
66 *Prorocentrum hoffmannianum* M. A. Faust and *P. lima* (Glibert *et al.* 2012).
67 Nevertheless, in the last years, other species that were previously considered as endemic
68 to certain areas have been reported in other regions, exhibiting an extremely disjunct
69 global distribution. This is the case of the epibenthic *Prorocentrum panamense* D.
70 Grzebyk, Y. Sako & B. Berland, which was identified and described from the waters of
71 Contadora Island on the Pacific coast of Panama in 1998, and since then, it has been
72 recorded in La Réunion (Indian Ocean), Martinique (Caribbean Sea), Revillagigedo
73 Islands (Mexican Pacific Ocean), and Hainan Island in the northern South China Sea (see
74 review in Chomérat *et al.* (2019)). In the past decade, several microalgae species
75 associated to toxin production have been newly recorded in the Canaries, and the majority
76 of them are dinoflagellates (Fraga *et al.* 2011; Rodríguez *et al.* 2018). In fact, the
77 particular position of the Canary Islands makes the archipelago a key point for marine
78 transport routes (Tichavska & Tovar 2015), and its peculiar environmental conditions
79 (Glibert *et al.* 2012) can facilitate the settlement of microalgae species introduced via
80 marine transport (Hallegraeff 1998). In this work, the first record of *P. panamense* in the
81 Canary Islands is reported, together with the toxicological characterization by LC-
82 MS/MS and neuro-2a cell-based assay (CBA).. This information is crucial to better
83 understand the global distribution, ecology and risks associated to species of the genus
84 *Prorocentrum*.

85 MATERIALS AND METHODS

86 Field sampling and microalgal cultures

87 Macroalgae samples were collected in April 2017 from three natural rock pools in Las
88 Salinas de Agaete (28°6'24.120"N, 15°42'40.140"W), Northwestern Gran Canaria (Fig.
89 1). Samples, of *ca.* 150–200 g fresh weight of macroalgae (fwm, hereafter) were
90 collected, placed in polystyrene bottles containing 1 L of seawater, vigorously shaken for
91 1 min to release epiphytic microalgae, and filtered (200- μ m mesh) to remove gross
92 material. From each sample, 100 mL were fixed in 3% of Lugol's iodine solution for
93 species identification and cell counting, and of the remaining 900 mL, 100 mL were used
94 for cells isolation purpose. Samples were kept at room temperature and close to a natural
95 source of light for a maximum of 3 days. Then, they were shipped to IRTA and stored in
96 the incubator (24°C) upon laboratory procedures. In the laboratory, cells were isolated
97 with a glass pipette under an inverted microscope (Leica, DMIL Pred LED) by the
98 capillary method (Stein *et al.* 1973), and cultivated in untreated Nunc 24 well plate
99 (Thermo Fisher Scientific) containing filtered and autoclaved local seawater (salinity
100 adjusted at 36 psu) supplemented with modified ES medium (Provasoli 1968). Cells were
101 grown at 24°C under a 12:12 light/dark cycle with a photon irradiance of 110 μ mol
102 photons $m^{-2} s^{-1}$. Once cultures reached approximately 20–35 cell mL^{-1} , they were
103 transferred to 28 mL round bottom glass tubes. After acclimation to laboratory conditions,
104 four 225 cm^2 cell culture flasks (500 mL volume, vented cap) were prepared with 150 cell
105 mL^{-1} each, from the same mother culture. Aliquots of cell cultures were stained with
106 Calco-fluor White M2R (Sigma Aldrich, Spain) (Fritz & Triemer 1985) and identified to
107 species level under an epifluorescence microscope (Leica, DMLB Condenser UCL).
108 Morphological features were determined according to Hoppenrath *et al.* (2013).
109 Microphotographs were taken with an Olympus DP-70 camera.

110 **Molecular analysis**

111 Molecular identification of the species was performed on genomic DNA isolated and
112 purified from 50 mL aliquots of cultures in the stationary phase, following the
113 phenol/chloroform procedure as described in Toldrà *et al.* (2018). The D1–D3 region of
114 the LSU rRNA gene was amplified by polymerase chain reaction (PCR) using the primers
115 D1R (5'-ACCCGCTGAATTTAAGCATA-3') and D2C (5'-
116 CCTTGGTCCGTGTTTCAAGA-3') (Chomérat *et al.* 2010). PCR was performed in a 25
117 μ L reaction containing 2.5 μ L of 1 \times PCR buffer, 1 μ L of 2 mM MgCl₂, 1.5 μ L of 600
118 μ M dNTPs, 0.25 μ L of each primer at a final concentration of 0.2 μ M, 0.20 μ L of 1 U
119 Taq DNA polymerase (Invitrogen™, Thermo Fisher™, Massachusetts, USA), 1.25 μ L of
120 5% dimethyl sulfoxide (DMSO), 2 μ L of template DNA at a concentration of 1 ng μ L⁻¹,
121 and sterile water to a final volume of 25 μ L. The PCR amplification was performed in a
122 Nexus Gradient Thermal Cycler (Eppendorf Ibérica, Madrid, Spain) for an initial
123 denaturation step of 94 °C for 5 min, followed by 40 cycles of 95°C for 30 s, 54°C for 30
124 s, and 72°C for 1 min, and then a final elongation step of 72°C for 5 min. Four μ L of each
125 PCR product were separated by electrophoresis (1% TAE, 60 V), stained with ethidium
126 bromide and checked under UV-illumination. PCR products were purified using a
127 Thermo Scientific GeneJET PCR purification Kit (Thermo Fisher™, Massachusetts,
128 USA) following manufacturer's instruction. The resulting purified product was
129 sequenced in both directions at Sistemas Genómicos (LLC, Valencia, Spain). Obtained
130 sequence was manually checked and edited using BioEdit v7.0.5.2 (Hall 1999). To assess
131 the evolutionary relationship between the obtained sequence and *Prorocentrum* species
132 sampled globally, we retrieved a set of 36 sequences belonging to 18 different species
133 from GenBank (see Fig. S1). *Adenoides eludens* (Herdman) Balech was used as outgroup.
134 Multiple sequence alignment was performed using MUSCLE algorithm implemented in

135 MEGA X (v10.0.5), and the phylogenetic relationships were estimated by
136 maximum likelihood (ML) using RaxML v.8 (Stamatakis 2014) and Bayesian inference
137 (BI) using MrBayes v.3.2.2 (Huelsenbeck & Ronquist 2001). Initial tree(s) for the
138 heuristic search were obtained automatically by applying neighbor-joining
139 and BioNJ algorithms to a matrix of pairwise distances estimated
140 using the maximum composite likelihood (MCL) approach, and then selecting the
141 topology with superior log likelihood value. A discrete Gamma distribution was used to
142 model evolutionary rate differences among sites (5 categories (+ G, parameter = 0.5083)).
143 Phylogenetic relationships were inferred by using the maximum likelihood method and
144 Tamura-Nei model. The rate variation model allowed for some sites to be evolutionarily
145 invariable. All positions containing gaps and missing data were eliminated.

146 **Toxin extraction**

147 Each of the four *Prorocentrum* replicates was harvested at four different phases of the
148 culture growth namely: latency phase (2 days, 225 cell mL⁻¹), exponential phase (14 days,
149 3650 cell mL⁻¹), beginning of the stationary phase (23 days, 5570 cell mL⁻¹), and end of
150 the stationary phase (34 days, 5390 cell mL⁻¹). Pellets were obtained by splitting the entire
151 bottle volume in 50 mL falcon tubes and centrifuging them at 3700 g for 25 min (Alegria
152 X-15R, Beckman Coulter). The obtained supernatants from each 50 mL tube were pooled
153 together according to the harvesting phase (the resulting fractions are referred as “culture
154 media” from here on). Both pellet and culture media from each harvesting phase were
155 analyzed for toxin presence. Cell pellets were extracted with 10 mL of pure methanol and
156 sonicated for 30 minutes (three times) at an amplitude of 37%, 3 sec on/2 sec off, using a
157 3 mm diameter sonicator probe (Watt ultrasonic processor VCX 750, Newton, USA). Cell
158 disruption after each sonication was evaluated under microscopy. Once solvent was
159 evaporated, the residue was re-suspended in 500 µL of methanol, vortexed, filtered with

160 a 0.2 μm PTFE filter, and transferred to autosampler vials. The culture media
161 corresponding to the four harvesting stages, instead, underwent a solid phase extraction
162 (SPE). Briefly, the entire volume of each harvested stage (500 mL) was filtered through an
163 Empore C18 disk (Sigma-Aldrich, Spain) to retain the toxins, which were afterwards
164 eluted with 10 mL of pure methanol. After solvent was evaporated, residue was re-
165 suspended in 500 μL of methanol, vortexed, filtered with 0.2 μm PTFE filter, and
166 transferred to autosampler vials. All samples were stored at -20°C until toxin analysis.

167 **LC-MS/MS analysis**

168 Certified reference materials (CRMs) of okadaic acid (OA), dinophysistoxin-1 (DTX-1),
169 dinophysistoxin-2 (DTX-2), yessotoxin (YTX), homoyessotoxin (hYTX), pectenotoxin-
170 2 (PTX-2), azaspiracid-1 (AZA-1), azaspiracid-2 (AZA-2), azaspiracid-3 (AZA-3), 13-
171 desmethylspirolide C (SPX-1), gymnodimine A (GYM-A) and pinnatoin G (PnTX-G)
172 were obtained from the National Research Council of Canada (NRC, Halifax, NS,
173 Canada). LC-MS/MS analysis of marine lipophilic toxins was performed following the
174 method described in García-Altare *et al.* (2013). Briefly, an Agilent 1200 LC (Agilent
175 Technologies, USA) was coupled to a 3200 QTRAP mass spectrometer (Applied
176 Biosystems, USA) through a TurboSpray[®] ion source operating at atmospheric pressure.
177 Toxins were separated on a XBridge BEH C8 2.5 μm 2.1 \times 50 mm column (Waters). A
178 binary gradient was programmed with water (mobile phase A) and acetonitrile/water
179 (mobile phase B), both containing 6.7 mM of ammonium hydroxide. All runs were carried
180 out at 30°C using a flow rate of $500 \mu\text{L min}^{-1}$. The injection volume was 10 μL and the
181 auto-sampler was set at 4°C . All lipophilic toxins were analyzed in both negative (-ESI)
182 and positive polarity (+ESI), selecting two product ions per toxin to allow the
183 quantification (the most intense transition) and confirmation; identification was supported
184 by toxin retention time and the multiple reaction monitoring (MRM) ion ratios. An

185 external standard calibration curve was prepared with a six-level curve, from 4 to 40 ng
186 toxin mL⁻¹ for OA. The minimum performance criteria were checked out throughout the
187 study such as retention time deviation ± 0.2 min, peak area deviation (RSD $\leq 3.0\%$),
188 linearity ($R^2 \geq 0.98$), sensitivity (individual toxin LOD should be equal or lower than
189 1:20th of regulatory level), precision intra-batch $\leq 20\%$ and inter-batch $\leq 25\%$. All
190 samples were analyzed in duplicate.

191 **Neuro-2a CBA**

192 CBA are routinely used to study the effect of bioactive compounds. In fact, the alteration
193 of homeostasis caused by these compounds, such as physiological cell disruption and cell
194 mortality, can be easily observed and measured. Indeed, CBA is commonly used for the
195 identification of marine toxins that affect food safety, including OA (see for instance
196 Diogène *et al.* 1995; Huynh-Delerme *et al.* 2003; Cañete & Diogène 2008). Experimental
197 conditions followed the procedures described in Cañete and Diogène (2008), with minor
198 modifications. Briefly, for the assay on the evaluation of cells morphology changes,
199 cultivated neuroblastoma neuro-2a cells were seeded into 96-well plates at an initial
200 density of 40,000 cells well⁻¹. After 24 h, cells were exposed to a 90 mM OA standard
201 solution (positive control), phosphate saline buffer (PBS, negative control), and the *P.*
202 *panamense* culture extracts (both microalgae pellets and culture media extracts) collected
203 at the four growing stages. Toxin standards and culture extracts were previously
204 evaporated to remove methanol completely, and subsequently re-suspended in a 5% fetal
205 bovine serum (FBS) medium. Then, samples were serially diluted, and initial pellet
206 extracts exposure concentrations were 1.0×10^4 (latency phase), 1.5×10^5 (exponential
207 phase), 2.0×10^5 (early stationary phase), and 1.8×10^5 cell equivalents mL⁻¹ (late
208 stationary phase) for the four harvested phases, respectively. Culture media extracts
209 exposure concentration was 2.4 mL culture media equivalents mL⁻¹ for the four phases.

210 After 4 h of exposure, the changes in cell morphology were observed under a light
211 microscope (Nikon Eclipse TE2000-S), and cells were photographed using phase
212 contrast. All conditions were tested in triplicate. In addition, a semi-quantitative
213 evaluation of *P. panamense* toxicity was performed following the CBA described by
214 Soliño *et al.* (2015). Cultivated neuro-2a cells were exposed to *P. panamense* pellets and
215 culture media extracts collected at the four harvested phases (4 serial ½ dilutions). Initial
216 pellet exposure concentrations for this test were 1.2×10^4 (latency phase), 1.7×10^5
217 (exponential phase), 2.4×10^5 (early stationary phase) and 2.1×10^5 cell equivalent/mL
218 (late stationary phase) for the four harvested phases, respectively. Initial culture media
219 extracts exposure concentration was 2.7 mL culture media equivalents mL⁻¹ for the four
220 phases. Cells were incubated for 24 h, and viability was assessed by the MTT (3-(4,5-
221 dimethylthiazol-2-yl)-2,5-diphenyltetrazolium bromide) assay (Manger *et al.* 1993). This
222 compound is converted to insoluble formazan crystals by mitochondrial dehydrogenase
223 activity. This activity can be performed only by live cells and results in a violet color that
224 can be measured by a spectrophotometer at 570 nm. All conditions were tested in
225 triplicate.

226 **RESULTS AND DISCUSSION**

227 **Molecular identification**

228 Isolated *Prorocentrum* cells presented the asymmetrical heart shaped form, asymmetrical
229 lateral plates and round posterior margin, and measured 46–52 µm in length and 43–46
230 µm in width (mean 49 µm and 44.5 µm respectively, n = 25) (Fig. 2), as originally
231 described by Grzebyk *et al.* (1998). Furthermore, calcofluor white stained cells showed
232 the reticulate-foveate thecal surface with depressions that become shallower towards the
233 plate center (Fig. 2). The internal part of this structure presents several pores, only visible
234 in the SEM image (Hoppenrath *et al.* 2013; Luo *et al.* 2017), and it is interpreted as a

235 synapomorphy of the *P. panamense* group. Most importantly, cells presented a large
236 sieve-like structure close to the thecal margin (Fig. 2A), a unique feature of *P. panamense*
237 and *P. pseudopanamense*. Stained cells also presented the linear periplagellar area (Fig.
238 2B), a typical trait of the *P. panamense* species. Finally, molecular analysis showed that
239 IRTA-SMM-17-72 (deposited in GenBank with the code MW600273) branches in a
240 subgroup of the other *P. panamense* species (Fig. S1). It must be underlined that there are
241 only 4 sequenced strains of *P. panamense*, three of them correspond to the same locality
242 (i.e., Martinique Island; IFR12-210, IFR12-212 and IFR12-218), and one from South
243 China Sea (TIO97). Thus, available data probably not represent the entire genetic
244 variance existing in the D1–D3 region of LSU rDNA. The only species that could arise
245 doubt about the correct species attribution of the strain described in this work is *P.*
246 *pseudopanamense* Chomérat & Nézan, since studies on the SSU rDNA showed that is
247 genetically close to *P. panamense* (Chomérat *et al.* 2011). Nevertheless, Chomérat *et al.*
248 (2019) stated that *P. panamense* species shape is very peculiar and morphologically easy
249 to recognize and it can be clearly distinguished from *P. pseudopanamense*, which is less
250 asymmetrical and never heart-shaped (Hoppenrath *et al.* 2013; Chomérat *et al.* 2019).

251 Knowledge of the ecology of benthic *Prorocentrum* species is very limited, and this is
252 due mostly to the difficulties to discriminate among them in benthic samples (Glibert *et*
253 *al.* 2012; Hoppenrath *et al.* 2013). Species of the dinoflagellate genus *Prorocentrum*
254 mainly occur in marine and brackish waters worldwide. Specifically, the type locality of
255 *P. panamense* is Contadora Island, on the Pacific side of the Gulf of Panama (Grzebyk *et*
256 *al.* 1998), but in the last decade its presence has been reported in La Réunion Island,
257 Martinique Island, Revillagigedo Islands (México), China, French Polynesia and in the
258 Arabian Gulf (Hansen *et al.* 2001; Hoppenrath *et al.* 2014; Gárate-Lizárraga & González-
259 Armas 2017; Chomérat *et al.* 2019). Thus, its presence in the Canary Islands is the first

260 record of *P. panamense* in the central eastern Atlantic Ocean. *Prorocentrum panamense*
261 exhibits an extraordinary disjunct global distribution pattern, with a low level of
262 intraspecific genetic variation in the LSU rDNA region (Chomérat *et al.* 2019).
263 Furthermore, the lack of previous records of this species in the Canary Islands is strongly
264 supported by recent surveys that failed to report the presence of the species in the region
265 (Fraga *et al.* 2011; Rodriguez *et al.* 2018). Although this absence may be due to species
266 misidentification, from a morphological perspective this species is very peculiar and easy
267 to recognize and identify (Chomérat *et al.* 2019). Thus, its presence in the region could
268 have happened naturally, we consider that a human-mediated introduction may be
269 occurred. The method of introduction is unknown, but the transport through ballast water
270 is considered the most probable vector of introduction. Coastal ship traffic constitutes an
271 effective introduction vector for aquatic organisms (Roy *et al.* 2012), and ballast water
272 from shipping has been considered responsible for the introduction of several benthic
273 dinoflagellate species in some countries (*e.g.*, Australia, Canada, Japan), sometimes with
274 dramatic economic consequences to aquaculture, fisheries and tourism (Hallegraeff 1998;
275 Roy *et al.* 2012). Ballast waters have been identified as a potential source for
276 dinoflagellate species introduction (Hallegraeff & Bolch 1992), and the Canary Islands
277 play an important role in the global marine transport. Las Palmas Port is a major logistic
278 platform between Europe, Africa and America, with a cargo hub over 19 million tons,
279 being a leading worldwide bunker trader (Tichavska & Tovar 2015). In addition, ballast
280 water from oil platforms have also suggested as a potential source of marine species
281 introduction to the Canary Islands (Brito *et al.*, 2011).

282 **Toxin content and profile**

283 The analysis on *P. panamense* extracts showed both the presence of toxic compounds and
284 toxicological activity. In fact, LC-MS/MS analysis showed the presence of OA in the

285 culture media extracted from the late stationary phase (Table S1, Fig. S2). No other
286 marine lipophilic toxins were found. Thus, this is the first record of toxin production of
287 *P. panamense*. The evaluation of cell morphology changes (neuro-2a) provided additional
288 information on the toxicity of the extracts (both from microalgae pellets and culture
289 media) obtained at the four different growth phases. Okadaic acid induces cell apoptosis
290 through the disruption of the filamentous actin (F-actin) cytoskeleton, the activation of
291 caspase-3 and the collapse of the mitochondrial membrane potential. This results in a
292 change in cell morphology and substrate detachment (Diogène *et al.* 1995; Cabado *et al.*
293 2004). In this work, morphological changes including cell blebbing and detachment could
294 be observed when control cells (Fig. 3A) were compared to the cells exposed to OA (Fig.
295 3B). After 4 h of incubation with the pellets and culture media extracts, neuro-2a cells
296 showed damages in presence of the pellet extract of *P. panamense* from late stationary
297 phase (Fig. 3C) and of the culture media extract of the early stationary phase (Fig. 3D).
298 Thus, even if OA was detected with LC-MS/MS only in the culture media extract of the
299 late stationary phase, neuro-2a cell anomalies showed the presence of OA-like toxicity in
300 other two extracts, underlying the toxic capacity of the *P. panamense* strain.

301

302 CBA results (Table S1) showed cell toxicity of all pellet extracts from the different
303 growth phases, with the exception of the latency phase. The cell mortality was as follow:
304 late stationary > early stationary > exponential. Furthermore, all culture media extracts
305 induced cell mortality, with a maximum in the early stationary phase and a minimum in
306 the exponential phase (early stationary > late stationary > latency > exponential). Hence,
307 it seems that the nature and/or concentration of toxic compounds released to the media
308 may vary not only according to the number of cells, and also to the phase of the growth.
309 These results confirmed the toxicity of *P. panamense* IRTA-SMM-17-72. In some

310 treatments a concomitant mortality evaluated by the MTT assay and morphological
311 changes in cells (e.g., early stationary phase) can be observed. Nonetheless, for some
312 treatments, cell mortality has been recorded but no morphological changes were
313 observed. This may be explained by the kinetics of the effects, and the time of
314 observation. It is also possible that changes in morphology end-up in cell detachment of
315 dead cells that would reduce the MTT signal, without observable changes in morphology.
316 Our results revealed the presence of OA and its effects on neuro 2a-cell morphology and
317 viability, in particular in the stationary phases with high concentrations of *P. panamense*
318 cells. Even if there are no studies investigating the cell growth and toxin production of *P.*
319 *panamense*, a similar toxin production behavior has been observed in the stationary phase
320 of some *P. lima* cultures (Bravo *et al.* 2001; Holmes *et al.* 2001). However, the results
321 derived from the analysis of *P. lima* showed a much higher OA contents (mean of 4.74
322 pg cell⁻¹ in Bravo *et al.* (2001) and 15 pg cell⁻¹ in Holmes *et al.* (2001)) compared to the
323 ones obtained in this work (Table S1). Even though, the CBA values related to OA-like
324 activity, obtained from the sum of pellet and culture media data, gives OA concentration
325 that are comparable with the ones obtained in the analysis of *P. lima* (Table S1). Only
326 Luo *et al.* (2017) investigated the toxicity of a *P. panamense* strain from China and
327 described it as non-toxic according to LC-MS/MS. However, in their work, cells were
328 collected during the mid-exponential phase, which also in our experiment show either
329 few (only with CBA) or a total absence of toxic activity or toxins. Thus, the undetected
330 toxicity of the Chinese strain could be related to the growth phase considered. Further
331 studies are needed to characterize the toxic profile of *P. panamense*, involving strains
332 from different regions.

333 **Conclusions**

334 *Prorocentrum panamense* strain was detected and identified in samples from Gran
335 Canaria (Canary Islands, Central Eastern Atlantic Ocean). This is the first record of this
336 species in the Macaronesian region and underlines the expansion of the *P. panamense*
337 distribution area. This discovery highlights the importance of monitoring programs and
338 long-term data sets, which facilitate the new detection of species. Additionally, in this
339 work, LC-MS/MS analysis confirmed the presence of OA, and the assay on the evaluation
340 of neuro-2a cell morphology changes together with the viability CBA with colorimetry,
341 identified the presence of OA-like activity in several extracts from both cell pellets and
342 culture media, pointing this species as a possible threat for human health. This is the first
343 toxicity report of a *P. panamense* strain. Hence, there is a need for further studies on the
344 toxicology of several strain belonging to this species to better assess the toxin production.
345 The identification of OA producing species out of their area of distribution can contribute
346 to the DSP risk assessment and help in spotting future outbreaks, so limiting the economic
347 cost associated to DSP events.

348 **Acknowledgments**

349 The research has received funding from the Ministerio de Ciencia e Innovación
350 (MICINN), the Agencia Estatal de Investigación (AEI), the European Food Safety
351 Authority through the EuroCigua project (GP/EFSA/AFSCO/2015/03) and the Fondo
352 Europeo de Desarrollo Regional (FEDER) through the CIGUASENSING (BIO2017-
353 87946-C2-2-R) project. The authors also acknowledge support from CERCA
354 Programme/Generalitat de Catalunya. G. Gaiani and À. Tudó acknowledge IRTA-
355 Universitat Rovira i Virgili for their PhD grant (2018PMF-PIPF-19 and 2016 PMF-PIPF-
356 74, respectively). The authors also acknowledge Margarita Fernández for sampling
357 support and Anna Safont for the LC-MS/MS technical work. The authors declare that

358 they have no known competing financial interests or personal relationships that could
359 have appeared to influence the work reported in this paper.

360

361 **References**

- 362 Aligizaki, K., Nikolaidis, G., Katikou, P., Baxevanis, A. D. and Abatzopoulos, T. J.,
363 2009. Potentially toxic epiphytic *Prorocentrum* (Dinophyceae) species in Greek
364 coastal waters. *Harmful Algae* **8**: 299-311.
- 365 Bravo, I., Fernández, M.L., Ramilo, I. and Martínez, A. 2001. Toxin composition of the
366 toxic dinoflagellate *Prorocentrum lima* isolated from different locations along
367 the Galician coast (NW Spain). *Toxicon* **39**: 1537-45.
- 368 Brito, A., Clemente, S. and Herrera, R. 2011. On the occurrence of the African hind,
369 *Cephalopholis taeniops*, in the Canary Islands (eastern subtropical Atlantic):
370 introduction of large-sized demersal littoral fishes in ballast water of oil
371 platforms? *Biol. Invasions* **13**: 2185-9.
- 372 Cabado, A. G., Leira, F., Vieytes, M.R., Vieites, J. M. and Botana, L. M. 2004.
373 Cytoskeletal disruption is the key factor that triggers apoptosis in okadaic acid-
374 treated neuroblastoma cells. *Arch. Toxicol.* **78**: 74-85.
- 375 Cañete, E. and Diogène, J. 2008. Comparative study of the use of neuroblastoma cells
376 (Neuro-2a) and neuroblastomaxglioma hybrid cells (NG108-15) for the toxic
377 effect quantification of marine toxins. *Toxicon* **52**: 541 -50.
- 378 Chomérat, N., Bilien, G. and Zentz, F. 2019. A taxonomical study of benthic
379 *Prorocentrum* species (Prorocentrales, Dinophyceae) from Anse Dufour
380 (Martinique Island, eastern Caribbean Sea). *Mar. Biodivers.* **49**: 1299-319.
- 381 Chomérat, N., Zentz, F., Boulben, S., Bilien, G., van Wormhoudt, A. and Nézan, E.
382 2011. *Prorocentrum glenanicum* sp. nov. and *Prorocentrum pseudopanamense*

383 sp. nov. (Prorocentrales, Dinophyceae), two new benthic dinoflagellate species
384 from South Brittany (northwestern France). *Phycologia* **50**: 202-14.

385 Chomérat, N., Sellos, D.Y., Zentz, F., and Nézan, E. 2010. Morphology and molecular
386 phylogeny of *Prorocentrum consutum* sp. nov. (Dinophyceae), a new benthic
387 dinoflagellate from South Brittany (Northwestern France). *J. Phycol.* **46**: 183-
388 94.

389 Diogène, G., Fessard, V., Dubreuil, A. and Puiseux-Dao, S. 1995. Comparative studies
390 of the actin cytoskeleton response to maitotoxin and okadaic acid. *Toxicol. in*
391 *Vitro* **9**:1-10.

392 Economou, V., Papadopoulou, C., Brett, M., *et al.* 2007. Diarrheic shellfish poisoning
393 due to toxic mussel consumption: The first recorded outbreak in Greece. *Food*
394 *Addit. Contam.* **24**: 297-305.

395 Fraga, S., Rodríguez, F., Caillaud, A., Diogène, J., Raho, N. and Zapata, M. 2011.
396 *Gambierdiscus excentricus* sp. nov. (Dinophyceae), a benthic toxic dinoflagellate
397 from the Canary Islands (NE Atlantic Ocean). *Harmful Algae* **11**: 10-22.

398 Fritz, L. and Triemer, R. E. 1985. A rapid simple technique utilizing calcofluor white
399 M2R for the visualization of dinoflagellate thecal plates 1. *J. Phycol.* **21**: 662-4.

400 Fujiki, H., Sukanuma, M., Yoshizawa, S., Nishiwaki, S., Winyar, B. and Sugimura, T.
401 1991. Mechanisms of action of okadaic acid class tumor promoters on mouse
402 skin. *Environ. Health. Perspect.* **93**: 211-14.

403 Gárate-Lizárraga, I. and González-Armas, R. 2017. First record of the dinoflagellate
404 *Prorocentrum panamense* (Prorocentrales, Dinophyceae) in the Mexican Pacific
405 from the Archipiélago de Revillagigedo. *CICIMAR Océánides* **32**: 63-6.

406 García-Altare, M., Diogène, J. and de la Iglesia, P. 2013. The implementation of liquid
407 chromatography tandem mass spectrometry for the official control of lipophilic

408 toxins in seafood: Single-laboratory validation under four chromatographic
409 conditions. *J. Chromatogr. A* **1275**: 48–60.

410 Gestal, C., Roch, P., Renault, T. *et al.* 2008. Study of diseases and the immune system
411 of bivalves using molecular biology and genomics. *Rev. Fish. Sci.* **16** (sup1):
412 133–56.

413 Glibert, P. M., Burkholder, J. M. and Kana, T. M. 2012. Recent insights about
414 relationships between nutrient availability, forms, and stoichiometry, and the
415 distribution, ecophysiology, and food web effects of pelagic and benthic
416 *Prorocentrum* species. *Harmful Algae* **14**: 231–59.

417 Grzebyk, D., Sako, Y. and Berland, B. 1998. Phylogenetic analysis of nine species of
418 *Prorocentrum* (Dinophyceae) inferred from 18S ribosomal DNA sequences,
419 morphological comparisons, and description of *Prorocentrum panamensis*, sp.
420 nov. *J. Phycol.* **34**: 1055–68.

421 Hall, T. A. 1999. BioEdit: a user-friendly biological sequence alignment editor and
422 analysis program for Windows 95/98/NT. *In* Nucleic acids symposium series.
423 Information Retrieval Ltd., c1979-c2000, London, pp. 95–98.

424 Hallegraeff, G. M. and Bolch, C. J. 1992. Transport of diatom and dinoflagellate resting
425 spores in ships' ballast water: implications for plankton biogeography and
426 aquaculture. *J. Plankton Res.* **14**: 1067–84.

427 Hallegraeff, G. M. 1998. Transport of toxic dinoflagellates via ships ballast water:
428 bioeconomic risk assessment and efficacy of possible ballast water management
429 strategies. *Mar. Ecol. Prog. Ser.* **168**: 297–309.

430 Hansen, G., Turquet, J., Quod, J. P. *et al.* 2001. Potentially harmful microalgae of the
431 western Indian Ocean: a guide based on a preliminary survey. IOC Manuals and
432 Guides 41, Intergovernmental Oceanographic Commission of UNESCO.

- 433 Holmes, M.J., Lee, F.C., Khoo, H.W. and Teo, S. L. M. 2001. Production of 7-deoxy-
434 okadaic acid by a New Caledonian strain of *Prorocentrum lima* (Dinophyceae).
435 *J. Phycol.* **37**: 280–8.
- 436 Hoppenrath, M., Chomérat, N., Horiguchi, T. Schweikert, M., Nagahama, Y. and
437 Murray, S. 2013. Taxonomy and phylogeny of the benthic *Prorocentrum* species
438 (Dinophyceae) –A proposal and review. *Harmful Algae* **27**: 1–28.
- 439 Hoppenrath, M., Murray, S. A., Chomérat, N. and Horiguchi, T. 2014. Marine Benthic
440 Dinoflagellates–Unveiling Their Worldwide Biodiversity. Senckenberg, Kleine
441 Senckenberg-Reihe, Germany.
- 442 Huelsenbeck, J. P. and Ronquist, F. 2001. MRBAYES: Bayesian inference of
443 phylogenetic trees. *Bioinformatics* **17**: 754–5.
- 444 Huynh-Delerme, C., Fessard, V., Kiefer-Biasizzo, H., and Puiseux-Dao, S. 2003.
445 Characteristics of okadaic acid-induced cytotoxic effects in CHO K1 cells.
446 *Environ. Toxicol.* **18**: 383–394
- 447 Luo, Z., Zhang, H., Krock, B., Lu, S., Yang, W. and Gu, H. 2017. Morphology,
448 molecular phylogeny and okadaic acid production of epibenthic *Prorocentrum*
449 (Dinophyceae) species from the northern South China Sea. *Algal Res.* **22**: 14–30.
- 450 Manger, R. L., Leja, L. S., Lee, S. Y., Hungerford, J. M. and Wekell, M. M. 1993.
451 Tetrazolium-based cell bioassay for neurotoxins active on voltage-sensitive
452 sodium channels: semiautomated assay for saxitoxins, brevetoxins, and
453 ciguatoxins. *Anal. Biochem.* **214**: 190–4.
- 454 Moreira-González, A.R., Fernandes, L.F., Uchida, H. *et al.* 2018. Variations in
455 morphology, growth, and toxicity among strains of the *Prorocentrum lima*
456 species complex isolated from Cuba and Brazil. *J. Appl. Phycol.* **31**: 519–32.

457 Provasoli, L. 1968. Media and prospects for the cultivation of marine algae, Cultures
458 and collection of algae, proceedings of the US-Japanese conference. Japan
459 Society of Plant Physiology, Hakone, pp. 63–75.

460 Rodriguez, F., Riobo, P., Crespin, G. D. *et al.* 2018. The toxic benthic dinoflagellate
461 *Prorocentrum maculosum* Faust is a synonym of *Prorocentrum hoffmannianum*
462 Faust. *Harmful Algae* **78**: 1–8.

463 Roy, S., Parenteau, M., Casas-Monroy, O., and Rochon, A. 2012. Coastal ship traffic: a
464 significant introduction vector for potentially harmful dinoflagellates in eastern
465 Canada. *Can. J. Fish. Aquat. Sci.* **69**: 627–44.

466 Soliño, L., Sureda, F.X. and Diogène, J. 2015. Evaluation of okadaic acid,
467 dinophysistoxin-1 and dinophysistoxin-2 toxicity on Neuro-2a, NG108-15 and
468 MCF-7 cell lines. *Toxicol. In Vitro* **29**: 59–62.

469 Stamatakis, A. 2014. RAxML version 8: a tool for phylogenetic analysis and post-
470 analysis of large phylogenies. *Bioinformatics* **30**: 1312–3.

471 Stein, J. R., Hellebust, J. A., and Craigie, J. S. 1973. Handbook of Phycological
472 Methods: Culture Methods and Growth Measurements. Cambridge University
473 Press, Cambridge.

474 Tichavska, M. and Tovar, B. 2015. Environmental cost and eco-efficiency from vessel
475 emissions in Las Palmas Port. *Transp. Res. E: Log. and Transp. Rev.* **83**: 126–
476 40.

477 Toldrà, A., Andree, K.B., Fernández-Tejedor, M. and Campàs M. 2018. Dual
478 quantitative PCR assay for identification and enumeration of *Karlodinium*
479 *veneficum* and *Karlodinium armiger* combined with a simple and rapid DNA
480 extraction method. *J. Appl. Phycol.* **30**: 2435–45.

481 Yasumoto, T., Murata, M., Oshima, Y., Sano, M., Matsumoto, G. K. and Clardy, J.
482 1985. Diarrhetic shellfish toxins. *Tetrahedron* **41**: 1019–25.

483

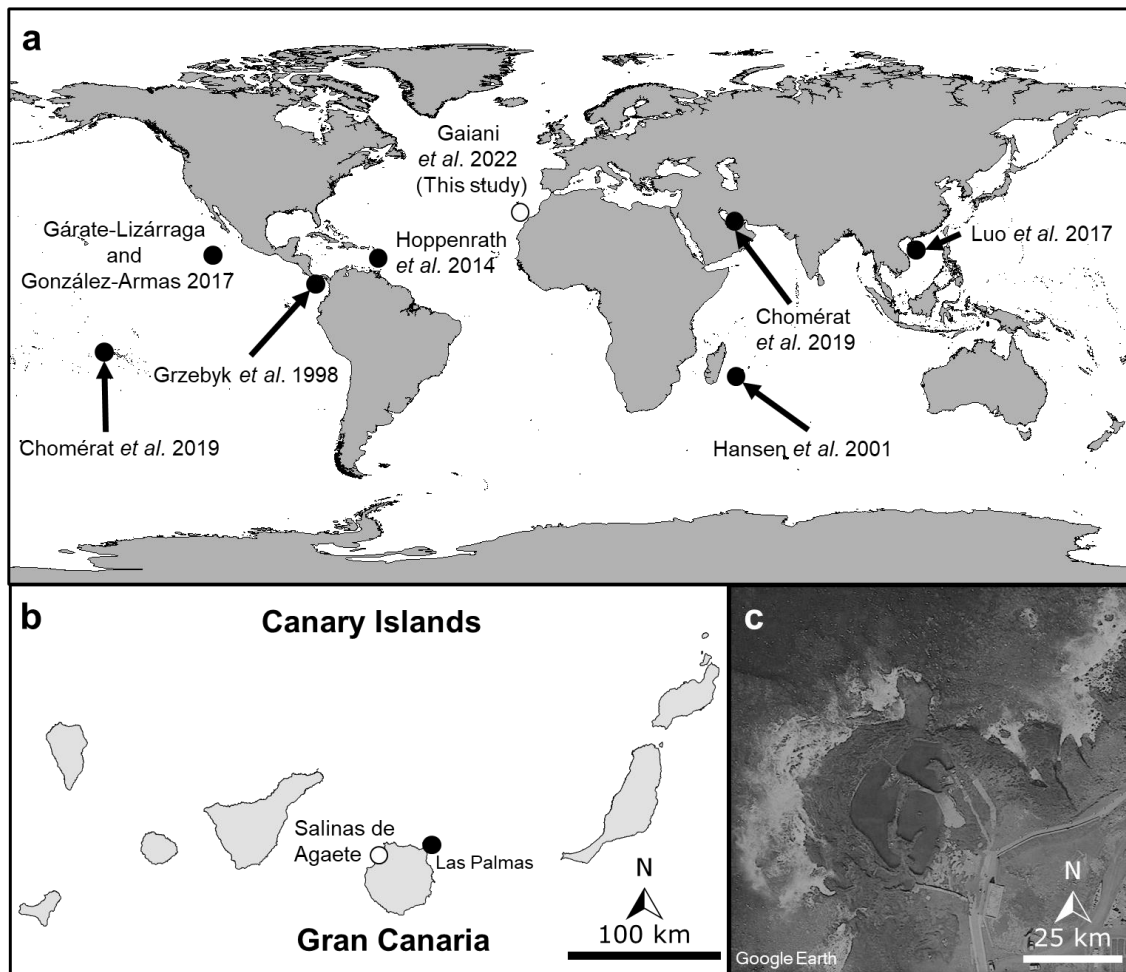
484 **Figure legends**

485 **Fig. 1.** Global distribution of *Prorocentrum panamense* (a). Black circles indicate
486 previous records. White circle indicates first record presented in this work.
487 Sampling site in Gran Canaria where *P. panamense* was found (Salinas de
488 Agaete) (b). © 2020 Google Earth vision of Salinas de Agaete (c).

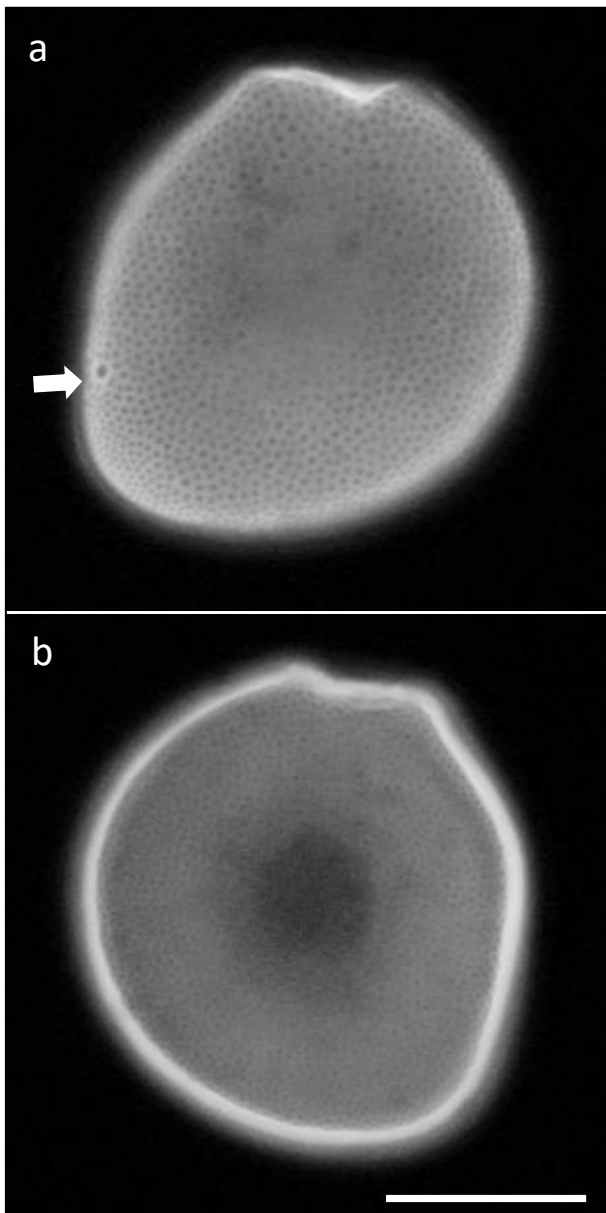
489 **Fig. 2.** Cell view of *Prorocentrum panamense* after calcofluor-white staining. It is
490 possible to observe the asymmetrical shape and reticulate-foveate thecal surface.
491 Left thecal view (a). Arrow indicates the marginal pore. Right thecal view (b).
492 Linear periflagellar area can be observed. Scale bar 20 µm.

493 **Fig. 3.** Morphology of neuroblasoma cells after 4 h exposure to PBS (control) (a),
494 okadaic acid at 90 nM (b), pellet extract from late stationary phase (c), and
495 culture media extract from early stationary phase (d). Scale bars 100 µm.

496



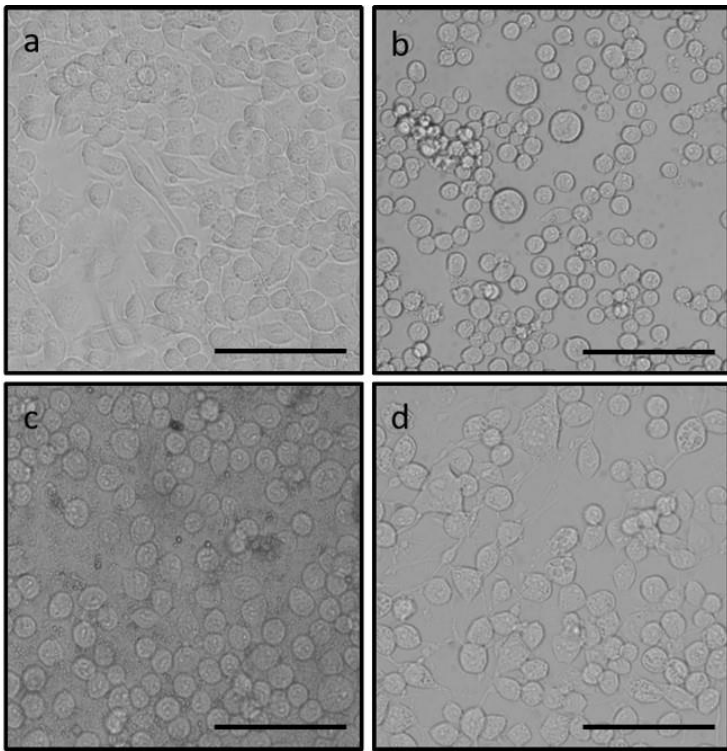
501 **Fig. 2.**



502

503

504 **Fig. 3**



505

506

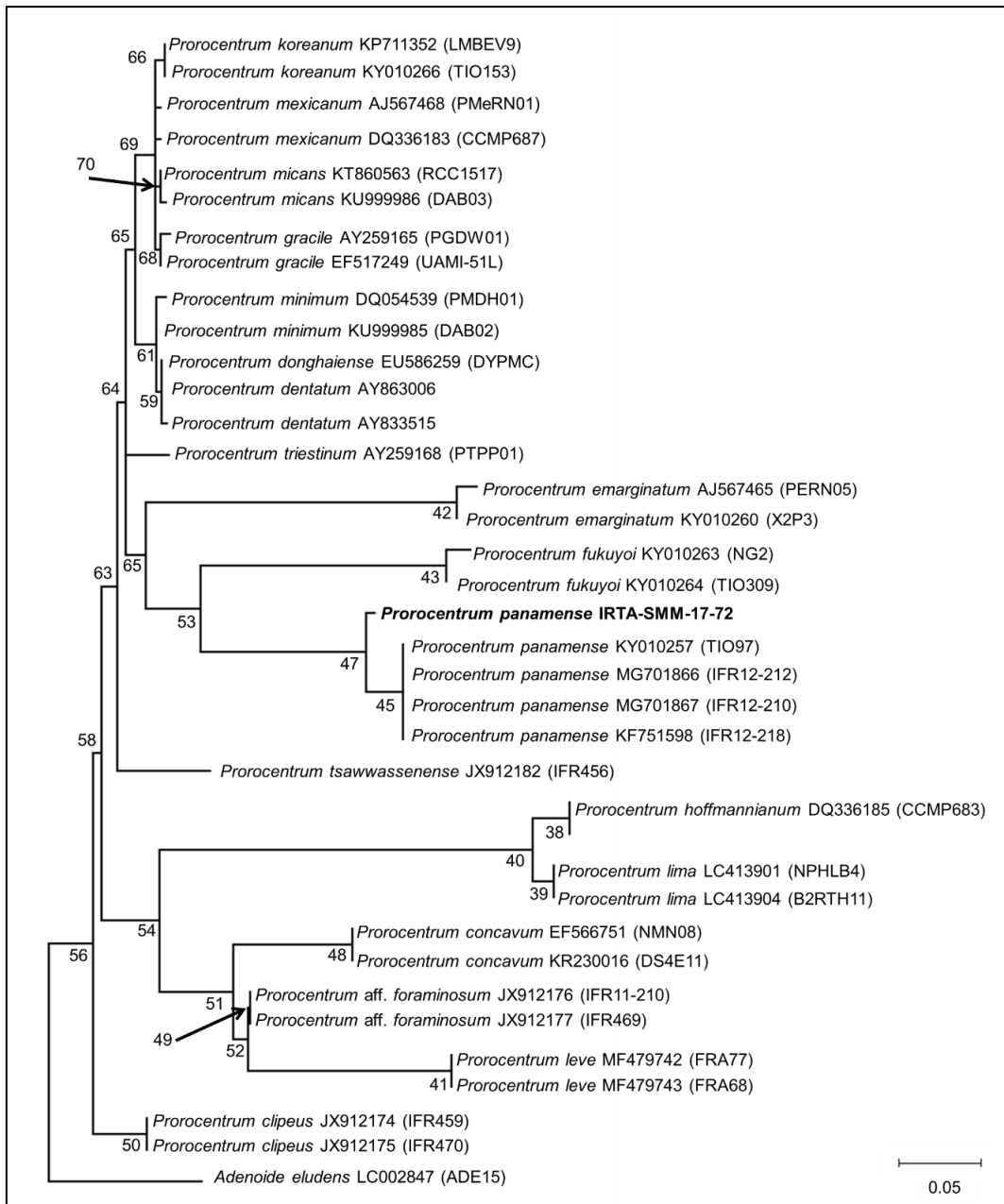
507

508 **Supporting information**509 **Table S1.** Comparison between CBA and LC-MS/MS toxicity results for the different culture phases.

Phase	cells/mL	Total cells	CBA			LC-MS/MS	
			Pellet	Culture media	Total	Pellet	Culture media
			OA	OA	OA	OA	OA
			(fg/cell)	(ng/mL)	(fg/cell)	(fg/cell)	(ng/L)
Latency (day 2)	225	1.13×10^5	< LOQ ^{a,b}	15.71 (IC ₅₀) ^b	43.61×10^3	< LOD ^d	< LOD ^e
Exponential (day 14)	3650	1.83×10^6	430.22 (IC ₅₀) ^b	7.01 (IC ₂₇) ^b	1.22×10^3	< LOD ^d	< LOD ^e
Early stationary (day 23)	5570	2.79×10^6	433.79 (IC ₅₀) ^c	36.05 (IC ₁₀₀) ^c	22.01×10^3	< LOD ^d	< LOD ^e
Late stationary (day 34)	5390	2.70×10^6	599.82 (IC ₅₀) ^c	22.97 (IC ₅₀) ^b	4.48×10^3	< LOD ^d	2.35

510 ^aLOQ CBA: 311-865 fg/cell in pellet, 6.2-13.8 ng/mL in culture media ; ^bno morphological affectation; ^cmorphological affectation. ^dLOD LC-
511 MS/MS in pellet : 0.14-3.64 fg/cell; ^eLOD LC-MS/MS in culture media: 0.80 ng/L

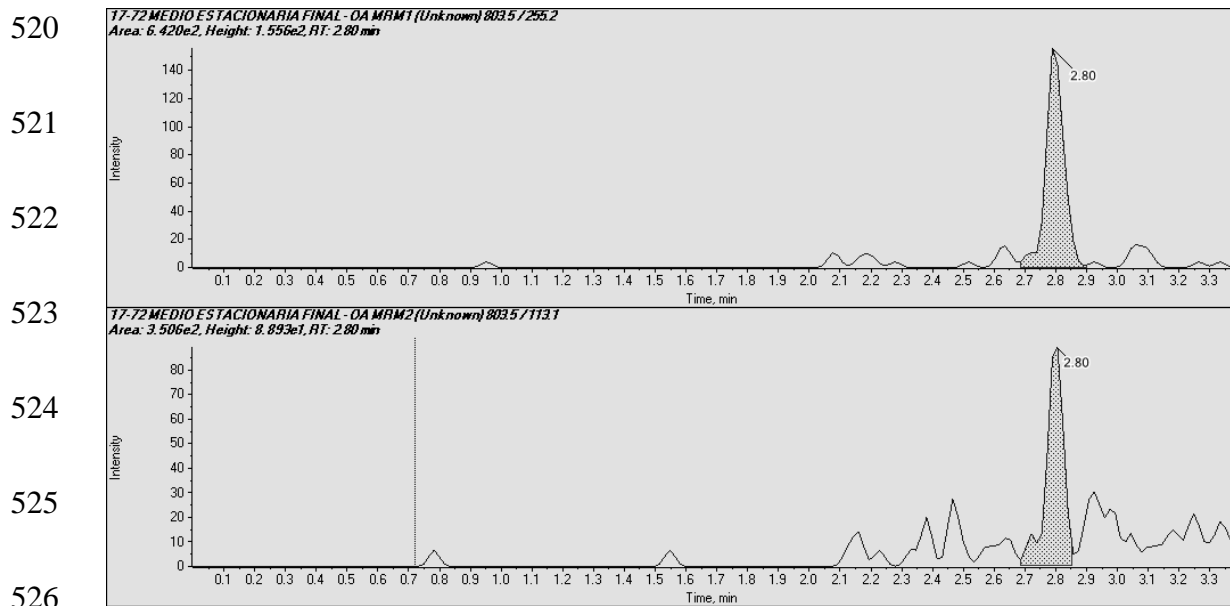
512



513

514 **Fig. S1.** Phylogenetic analysis of LSU 28S rDNA gene of the available *Prorocentrum*
515 sequences (GenBank) and *P. panamense* collected in this study (in bold). The tree with
516 the highest log likelihood is shown (-2071.16). Values at nodes are bootstrap values
517 obtained by the maximum likelihood method. Bootstrap values less than 30 % are not
518 shown.

519



527 **Fig. S2.** Multiple reaction monitoring chromatogram of transitions monitored obtained
528 following the analysis of OA in the late stationary culture media by LC-MS/MS.

529

530

531